Terr. Atmos. Ocean. Sci., Vol. 18, No. 3, 567-576, August 2007

Effect of Finite Frequency Bandwidth Limitation on Evaluations of Seismic Radiation Energy of the 1999 Chi-Chi Earthquake

Jeen-Hwa Wang[1, *] and Ming-Wey Huang [2, 3]

(Manuscript received 23 June 2006, in final form 15 January 2007)

ABSTRACT

Based on the ω^{-2} and ω^{-3} source models, we explore the effect on estimates of seismic radiation energy, E_s, caused by finite frequency bandwidth limitation of source spectra. Let f_c be the corner frequency of a source spectrum and f_u and f_c are, respectively, the upper and lower bounds of a frequency band in use. Results show that the effect depends on f_u/f_c and f_l/f_c, and E_s is under-estimated when $f_l > 0$ and $f_u < \infty$. When $f_u/f_c < 20$, the effect is sensitive to both f_l/f_c and f_u/f_c for the ω^{-2} source model, but mainly to f_l/f_c for the ω^{-3} model. When $f_u/f_c > 20$, the effect is insensitive only to f_u/f_c for the two models. Let E_s' be the seismic radiation energy estimated without removal of finite frequency bandwidth limitation. Results show: (1) E_s'/E_s first slightly increases and then decreases with increasing f_c; or (2) E_s'/E_s monotonously decrease with increasing f_c. For the 1999 M_s 7.6 Chi-Chi earthquake, Taiwan, E_s was under-estimated by Hwang et al. (2001), and the degree of under-estimates varies from station to station.

(Key words: Seismic radiation energy, Corner frequency, Finite frequency bandwidth limitation)

1. INTRODUCTION

Seismic radiation energy, E_s, is an important parameter quantifying an earthquake (cf. Wang 2006). However, estimates of E_s can be influenced by the source spectrum, seismic

[1] Institute of Earth Sciences, Academia Sinica, Taipei, Taiwan, ROC
[2] Institute of Geophysics, National Central University, Chung-Li, Taiwan, ROC
[3] National Science and Technology Center for Disaster Reduction, Taipei, Taiwan, ROC
[*] *Corresponding author address:* Dr. Jeen-Hwa Wang, Institute of Earth Sciences, Academia Sinica, Taipei, Taiwan, ROC; E-mail: jhwang@earth.sinica.edu.tw
doi: 10.3319/TAO.2007.18.3.567(T)

radiation patterns, seismic-wave attenuation, surface amplification, site effect, instrumental response, and noise. A correct evaluation of E_s will help seismologists to understand source behavior more exactly. Boore (1988), Di Bona and Rovelli (1988), and Singh and Ordaz (1994) stressed that E_s is underestimated when high-frequency signals are not included. Thus, the E_s measured from local seismograms is usually larger than that done from teleseismic data (Bolt 1986; Smith et al. 1991; Singh and Ordaz 1994; Hwang et al. 2001; Huang et al. 2002). In principle, E_s is measured for f = 0 - ∞ Hz, while in practice the measurement can be made only for $f_l \leqq f \leqq f_u$ due to limitation in instrumental response and noise. This results in so-called finite frequency bandwidth limitation (denoted *ffbl* hereafter). Ide and Beroza (2001) theoretically studied such an effect in a high-frequency regime. Based on the ω^{-2} source model, Wang (2004) studied the effect in both low- and high-frequency regimes. Both studies show underestimation of E_s due to the *ffbl*-effect.

For the 1999 M_s 7.6 Chi-Chi earthquake, Wang (2004) made corrections only based on the ω^{-2} source model. However, Huang and Wang (2002) stressed that a ω^{-3} model must be taken into account for the northern fault plane of the earthquake. In this work, the *ffbl*-effects of source spectrum for both high- and low-frequency regimes on estimates of E_s based on the ω^{-2} and ω^{-3} source models (Aki 1967; Brune 1970) will be discussed in detail. Theoretical results will be applied to correct estimates of the seismic radiation energy of the Chi-Chi earthquake.

2. DEFINITION AND METHODOLOGY FOR MEASURING E_S

The source spectra of earthquakes are mainly controlled by the low-frequency spectral level (Ω_o) and corner frequency (f_c) (Aki 1967). Theory and observations show that when $f > f_c$, the spectral amplitude decays in a power-law function like $f^{-\alpha}$. Commonly accepted power-law functions have either f^{-2} or f^{-3}, which are, respectively, referred to as the ω^{-2} and ω^{-3} source models, where $\omega = 2\pi f$ (Aki 1967; Brune 1970).

Let d(t) and v(t) be the source displacement and velocity, respectively. Their Fourier transforms are, respectively, D(f) and V(f). D(f) can be approximated by $D_2(f) = \Omega_o/[1+(f/f_c)^2]$ for the ω^{-2} model and $D_3(f) = \Omega_o/[1+(f/f_c)^2]^{3/2}$ for the ω^{-3} one (cf. Beresnev and Atkinson 1997). Hence, the approximations of V(f) are, respectively:

$$V_2(f) = 2\pi f\Omega_o/[1+(f/f_c)^2] \quad , \tag{1}$$

$$V_3(f) = 2\pi f\Omega_o/[1+(f/f_c)^2]^{3/2} \quad . \tag{2}$$

As $f << f_c$, $V_2(f) \sim f^1$ and $V_3(f) \sim f^1$, while as $f >> f_c$, $V_2(f) \sim f^{-1}$ and $V_3(f) \sim f^{-2}$. Eqs. (1) ~ (2) can be approximated individually by a piece-wise linear function (Fig. 1).

E_s is calculated by the following expression:

$$E_s = 4\pi\rho\beta \int v^2(t)dt = 4\pi\rho\beta[2\int V^2(f)df] \quad , \tag{3}$$

where ρ and β are, respectively, the density and the S-wave velocity. In principle, the first integral is performed from $-\infty$ to $+\infty$ in the time domain and the second one from 0 to $+\infty$ in the frequency domain. Define:

$$I_V = \int v^2(t)dt = 2\int V^2(f)df \quad . \tag{4}$$

Thus, $E_s = 4\pi\rho\beta I_V$.

3. THE EFFECT DUE TO FINITE FREQUENCY BANDWIDTH LIMITATION

Wang (2004) derived the formulas to show the *ffbl*-effect based on the ω^{-2} model. For the purpose of comparison, his formulas are shown again below. In the following, we add a subscript 'o' to denote a quantity obtained through integration from $-\infty$ and $+\infty$ sec in the time domain or from 0 to ∞ Hz in the frequency domain. Inserting Eqs. (1) and (2) into Eq. (4), respectively, leads to:

$$I_{V2o} = I_V(f_l = 0,\ f_u = \infty) = \Omega_o^{\ 2}(2\pi f_c)^3/4 \quad , \tag{5}$$

$$I_{V3o} = I_V(f_l = 0,\ f_u = \infty) = \Omega_o^{\ 2}(2\pi f_c)^3/16 \quad , \tag{6}$$

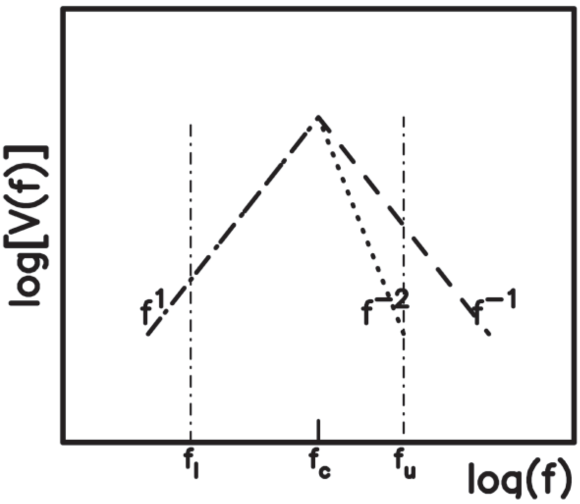

Fig. 1. The log-log plots of the normalized, simplified velocity spectra, V(f) versus frequency, f: the dashed and dotted lines, respectively, for the f^{-1} and f^{-2} source velocity models. The two vertical dashed-dotted lines display the frequency band in use.

where the subscript is 2 for the ω^{-2} model and 3 for the ω^{-3} model. Clearly, $I_{V2o} = 4I_{V3o}$. When integration is made only in a finite frequency band from f_l to f_u, with $f_l < f_c < f_u$, which is in between two dashed-dotted lines as shown in Fig. 1, the *ffbl*-effect exists. When $f_c/f_l = f_u/f_c$, for the ω^{-2} model the high-frequency cut-off part with $f > f_u$ is almost equal to that from the low-frequency one with $f < f_l$; while for the ω^{-3} model the former is smaller than the latter.

Inserting Eqs. (1) and (2) into Eq. (4), with $f_l < f_c < f_u$, respectively, gives:

$$I_{V2} = 2\Omega_o^2 \int (2\pi f)^2 [1+(f/f_c)^2]^{-2} df \quad , \tag{7}$$

$$I_{V3} = 2\Omega_o^2 \int (2\pi f)^2 [1+(f/f_c)^2]^{-3} df \quad , \tag{8}$$

where the integral range is of from f_l to f_u. After integration, Eqs. (7) and (8), respectively, becomes:

$$I_{V2} = I_{V2o} F_{V2} \quad , \tag{9}$$

$$I_{V3} = I_{V3o} F_{V3} \quad , \tag{10}$$

where

$$F_{V2} = (2/\pi)\{-(f_u/f_c)/[1+(f_u/f_c)^2] + (f_l/f_c)/[1+(f_l/f_c)^2] + \tan^{-1}(f_u/f_c) - \tan^{-1}(f_l/f_c)\} \quad , \tag{11}$$

$$\begin{aligned} F_{V3} = (4/\pi)\{&-(f_u/f_c)/[1+(f_u/f_c)^2]^2 + (f_u/f_c)/2[1+(f_u/f_c)^2] + \tan^{-1}(f_u/f_c)/2 \\ &+ (f_l/f_c)/[1+(f_l/f_c)^2]^2 - (f_l/f_c)/2[1+(f_l/f_c)^2] - \tan^{-1}(f_l/f_c)/2\} \quad . \end{aligned} \tag{12}$$

When $f_l = 0$ and $f_u \rightarrow \infty$, $F_{V2} = 1$ and $F_{V3} = 1$, and, thus, $I_{V2} = I_{V2o}$ and $I_{V2} = I_{V3o}$.

Hereafter, let E_s and E_s' be the values of seismic radiation energy estimated, respectively, with and without removal of the *ffbl*-effect. From Eqs. (9) - (12), the energy ratio of E_s' to E_s is:

$$E_{s2}'/E_s = F_{V2} \quad , \tag{13}$$

for the ω^{-2} model and:

$$E_{s3}'/E_s = F_{V3} \quad , \tag{14}$$

for the ω^{-3} model. The variations of E_{s2}'/E_s and E_{s3}'/E_s with f_l/f_c are made only for $f_l/f_c < 1$ and $f_l/f_c > 1$ under the request of $f_l < f_c < f_u$. In other words, the calculations are made when $f_l/f_c = 0.05$ - 0.95 and $f_u/f_c = 2$ to 20, with a difference of 2. The plots for ten values of f_u/f_c are shown, respectively, in Fig. 2 (for E_{s2}'/E_s) and Fig. 3 (for E_{s3}'/E_s), where the dotted line displays the energy ratio of 1, without *ffbl*.

In Figs. 2 and 3, all curves are below the dotted line with $E_s'/E_s = 1$, and, thus, E_{s2}'/E_s and E_{s3}'/E_s are both smaller than 1, with a maximum of about 0.937 for E_{s2}'/E_s and 0.999 for E_{s3}'/E_s. Obviously, the *ffbl*-effect yields an under-estimation of seismic radiation energy. E_{s2}'/E_s and

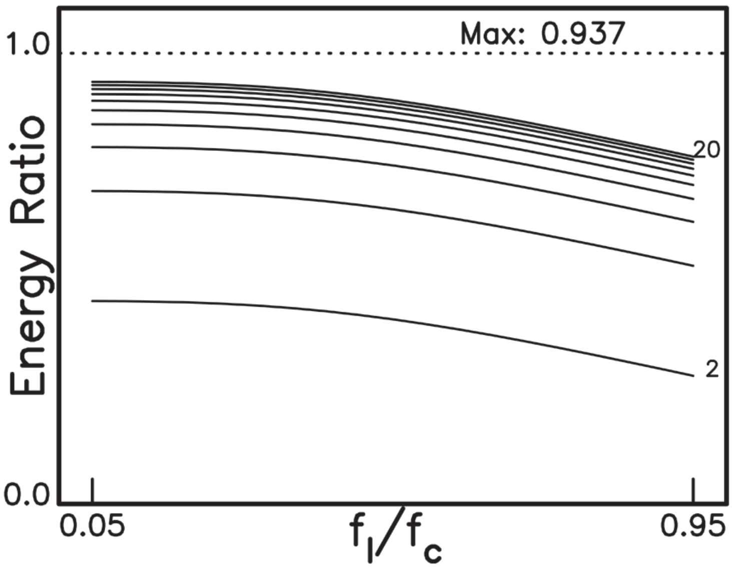

Fig. 2. The variations of E_{s2}'/E_s with f_l/f_c (from 0.05 to 0.95) for ten values of f_u/f_c (from 2 to 20). The dotted line represents E_{s2}'/E_s = 1.

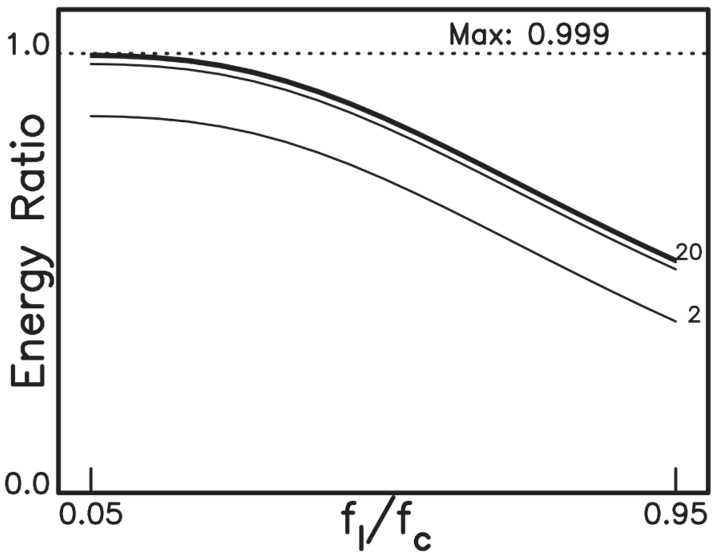

Fig. 3. The variations of E_{s3}'/E_s with f_l/f_c (from 0.05 to 0.95) for ten values of f_u/f_c (from 2 to 20). The dotted line represents E_{s3}'/E_s = 1.

E_{s3}'/E_s both decrease with increasing f_l/f_c, and the amount of the decreasing rate increases with f_l/f_c. For fixed f_c, decreases in E_{s2}'/E_s and E_{s3}'/E_s with increasing f_l/f_c lead to increases in E_{s2}'/E_s and E_{s3}'/E_s with decreasing f_l. This indicates that an increase in the width of the low-frequency regime improves estimation of E_s. When $f_l/f_c < 0.4$ for E_{s2}'/E_s and $f_l/f_c < 0.2$ for E_{s3}'/E_s, the curves are almost flat for all f_u/f_c. This means that $f_l = 0.4f_c$ for E_{s2}'/E_s and $f_l = 0.2f_c$ for E_{s3}'/E_s are the individual optimum lower bounds to lead to a stable value of E_s.

E_{s2}'/E_s and E_{s3}'/E_s both increase with f_u/f_c. The curves are close to one another for E_{s2}'/E_s when $f_u/f_c \geqq 10$ and for E_{s3}'/E_s when $f_u/f_c \geqq 4$, thus indicating that $f_u = 10f_c$ for E_{s2}'/$E_s$and $f_u = 4f_c$ for E_{s3}'/E_s are both large enough to lead to a stable estimate of E_s. For fixed f_c, increases in E_{s2}'/E_s and E_{s3}'/E_s with f_u/f_c yield increases in E_{s2}'/E_s and E_{s3}'/E_s with f_u, thus indicating that an increase in the width of high-frequency regime improves estimates of E_s. This is consistent with others' (Boore 1988; Di Bona and Rovelli 1988; Singh and Ordaz 1994; Ide and Beroza 2001).

Figures. 2 and 3 show that for fixed f_l, decreases in E_{s2}'/E_s and E_{s3}'/E_s with increasing f_l/f_c lead to increases in E_{s2}'/E_s and E_{s3}'/E_s with f_c, thus implying that the *ffbl*-effect in the low-frequency regime gives a greater underestimate of E_s for events with lower f_c than for those with higher f_c. This effect is stronger for the ω^{-3} model than the ω^{-2} model. For fixed f_u, increases in E_{s2}'/E_s and E_{s3}'/E_s with f_u/f_c result in increases in E_{s2}'/E_s and E_{s3}'/E_s with decreasing f_c, thus showing that the *ffbl*-effect in the high-frequency regime yields a bigger underestimate of E_s for events with higher f_c than for those with lower f_c. When both f_l and f_u are finite and fixed, an increase in f_c will lead to a decrease in both f_l/f_c and f_u/f_c. Hence, the variation of E_{s2}'/E_s and E_{s3}'/E_s with f_c can be either of the following two types: (1) the ratio first slightly increases and then decreases with increasing f_c; and (2) the ratio monotonously decrease with increasing f_c.

4. RE-EVALUATION OF E_S OF THE 1999 CHI-CHI EARTHQUAKE

The M_s 7.6 Chi-Chi earthquake, which ruptured the Chelungpu fault, struck central Taiwan on 20 September 1999. The epicenter and the fault trace are displayed in Fig. 4. The values of f_c and Ω_o at four near-fault stations evaluated by Hwang et al. (2001) are $f_c = 0.064$ - 0.193 Hz and $\Omega_o = 89.4$ - 2350.0 cm. The values of f_c and Ω_o are shown in columns 2 and 3 of Table 1. They also estimated the values of E_s, which is equivalent to E_{s2}' for the ω^{-2} model and E_{s3}' for the ω^{-3} source model in this study and denoted by E_s' in column 8 of Table 1, at four near-fault seismic stations (see Fig. 4) based on two sets of f_l and f_u: (1) $f_l = 0.03$ and $f_u = 1.0$ Hz at TCU102 and TCU052; and (2) $f_l = 0.03$ and $f_u = 3.0$ Hz at TCU076 and TCU129. The values of f_l and f_u used are shown in columns 4 and 5 of Table 1. In order to obtain a reliable value of E_s, they eliminated the effects caused by seismic radiation patterns, seismic-wave attenuation, surface amplification, site effect, and instrumental response. Wang (2004) re-evaluated the values of E_s estimated by Hwang et al. (2001) through the removal of the *ffbl*-effect based on the ω^{-2} model. His values of E_{s2}'/E_s and Es are shown in parentheses of columns 9 and 10 in Table 1.

From the values of f_c, f_l, and f_u at the four stations, the ratios of f_l/f_c and f_u/f_c are calculated and given in column 6 and 7 of Table 1: f_l/f_c of from 0.155 to 0.469 and f_u/f_c of from 8.197 to

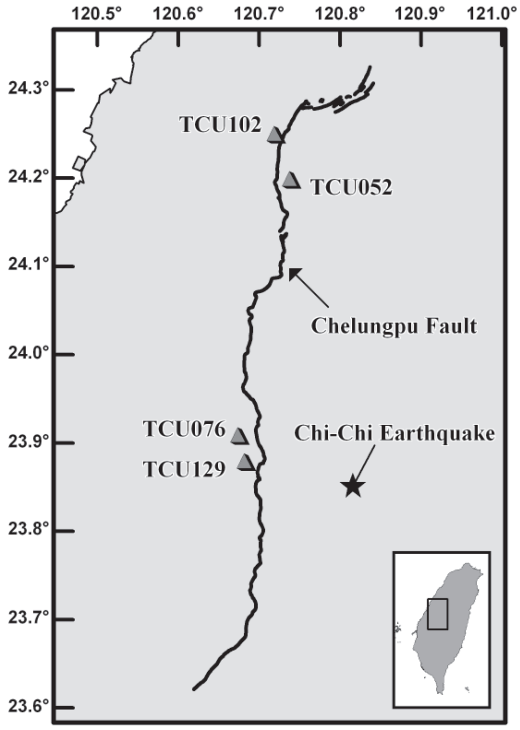

Fig. 4. A map showing the epicenter (in a solid star) of the 1999 Chi-Chi earthquake, the Chelungpu fault (in a solid line), and four near-fault seismic stations (in solid triangles).

Table 1. The values of several parameters at four near-fault seismic stations. In columns 9 and 10, E_s'/E_s and E_s, respectively, includes E_{s2}'/E_s and E_s for the ω^{-2} model and E_{s3}'/E_s and E_s for the ω^{-3} model. The values of E_s'/E_s and E_s not inside the parenthesis are, respectively, E_{s2}'/E_s and E_s taken from Wang (2004). The values of E_s'/E_s and E_s inside the parenthesis are, respectively, E_{s3}'/E_s and E_s of this study.

Stations	**f_c (Hz)**	**Ω_o (cm)**	**f_l (Hz)**	**f_u (Hz)**	**f_l/f_c**	**f_u/f_c**	**E_s' (ergs)**	**E_s'/E_s**	**E_s (erg)**
TCU102	0.122	551.2	0.03	1.0	0.246	8.197	9.7×10^{22}	0.840 (0.974)	1.2×10^{23} (9.9×10^{22})
TCU052	0.064	2350.0	0.03	1.0	0.469	15.625	2.5×10^{23}	0.884 (0.877)	2.8×10^{23} (2.9×10^{23})
TCU076	0.193	89.4	0.03	3.0	0.155	15.544	1.0×10^{22}	0.917	1.1×10^{22}
TCU129	0.160	105.0	0.03	3.0	0.188	18.750	6.7×10^{21}	0.929	7.2×10^{21}

18.750. The values of E_{s2}'/E_s and E_s re-evaluated by Wang (2004) based on the ω^{-3} model are shown in the parentheses of columns 9 and 10 in Table 1. Clearly, the *ffbl*-effect results in an underestimate of E_s, and the underestimate is higher at two northern stations than at the southern ones. We calculate the values of E_s'/E_s and E_s at two northern stations using Eqs. (12) and (13) based on the ω^{-3} model. Results are shown in the parentheses of columns 9 and 10 of Table 1. Obviously, the results are opposite to those evaluated based on the ω^{-2} model. The difference is bigger at TCU102 and smaller at TCU052. Based on the ω^{-3} model, the value of E_s at TCU102 estimated by Hwang et al. (2001) is good enough.

To examine the problem in advance, we plot the variations of energy ratio with f_c in the range 0.05 - 0.20 Hz in Fig. 5 for two sets of f_l and f_u: (1) $f_l = 0.03$ and $f_u = 1.0$ Hz for northern seismic stations; and (2) $f_l = 0.03$ and $f_u = 3.0$ Hz for southern ones. The dashed and solid lines represent, respectively, E_{s2}'/E_s and E_{s3}'/E_s for the northern stations; and the dashed-dotted line shows E_{s2}'/E_s for the southern stations. The estimated results are also plotted by an open circle or a cross attached with a station code in Fig. 5.

In Fig. 5, E_{s2}'/E_s first increases and then decreases with increasing f_c. Whereas, E_{s3}'/E_s first increases with f_c and then becomes flat when $f_c > 0.14$ Hz. The variations are as expected as mentioned above. The three variations are all below the dotted line with E_s'/$E_s = 1$, thus showing underestimate of E_s at the four seismic stations. The solid line intersects the dashed

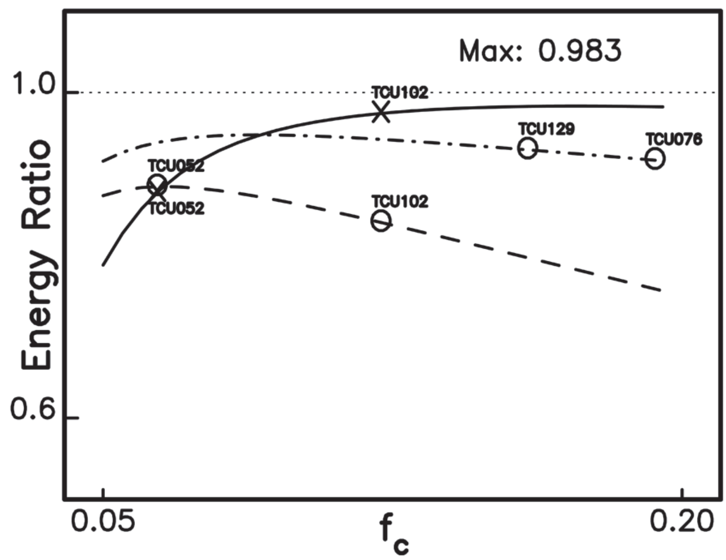

Fig. 5. The variations of energy ratio with f_c for various values of f_l and f_u as mentioned in the text: the dashed and solid lines, respectively, for E_{s2}'/E_s and E_{s3}'/E_s at the northern stations, and the dashed-dotted line for E_{s2}'/E_s at the southern ones. The related values at four near-fault seismic stations for the Chi-Chi earthquake are displayed by an open circle or a cross attached with a station code. The dotted line represents E_s'/$E_s = 1$.

and dashed-dotted ones at $f_c = 0.065$ and $f_c = 0.090$ Hz, respectively. Hence, at the northern stations the underestimate of E_s is smaller from the ω^{-2} model than from the ω^{-3} model when $f_c < 0.065$ Hz, and opposite when $f_c > 0.065$ Hz. The difference between the effects from the two models is small at TCU052 and large at TCU102. Underestimation of E_s is smaller at the southern stations than at the northern ones when $f_c < 0.09$ Hz, and opposite when $f_c > 0.09$ Hz. Consequently, the values of E_s at the four near-fields suggested by this study are 9.9×10^{22} erg at TCU102, 2.9×10^{23} erg at TCU052, 1.1×10^{22} erg at TCU076, and 7.2×10^{21} erg at TCU129.

5. CONCLUSION

The *ffbl*-effect of source spectrum on estimation of seismic radiation energy, E_s, is analyzed theoretically on the basis of the ω^{-2} and ω^{-3} source models. Such an effect depends on f_l/f_c and f_u/f_c. Numerical results obviously show that E_s are underestimated for all f_l/f_c and f_u/f_c. An increase in the frequency bandwidth including either the high- or low-frequency regime will increase reliability of estimating E_s. When $f_u/f_c < 20$, the effect is sensitive to both f_l/f_c and f_u/f_c for the ω^{-2} model, but mainly to f_l/f_c for the ω^{-3} model. When $f_u/f_c > 20$, the effect is insensitive to f_u/f_c for the two models. For the two source models, E_s'/E_s depends on f_c in either: (1) E_s'/E_s first slightly increases and then decreases with increasing f_c; or (2) E_s'/E_s monotonously decreases with increasing f_c. Numerical results also suggest that Fig. 2 or 3 together with Fig. 5 can help us to select an appropriate frequency band for estimating a reliable value of seismic radiation energy. The values of f_l and f_u leading to an optimum estimate of E_s are $f_l = 0.4f_c$ and $f_u = 10f_c$ for the ω^{-2} model and $f_l = 0.2f_c$ and $f_u=4f_c$ the ω^{-3}model.

For the 1999 M_s 7.6 Chi-Chi, Taiwan, earthquake, the revised values of E_s show that E_s was underestimated by Hwang et al. (2001). However, the degree of underestimates varies from station to station. At the northern stations underestimation of E_s is smaller for the ω^{-2} model than for the ω^{-3} model when $f_c < 0.065$ Hz, and opposite when $f_c > 0.065$ Hz. The difference between the effects from the two models is small at TCU052 and large at TCU102. Underestimation of E_s is smaller at the southern stations than at the northern ones when $f_c < 0.09$ Hz, and opposite when $f_c > 0.09$ Hz. The values of E_s at the four near-field are 9.9×10^{22} erg at TCU102, 2.9×10^{23} erg at TCU052, 1.1×10^{22} erg at TCU076, and 7.2×10^{21} erg at TCU129.

Acknowledgements The authors would like to express their thanks to two reviewers for valuable comments and suggestions. The study was financially supported by Academia Sinica and the National Sciences Council under Grant No. NSC94-2119-M-001-012.

REFERENCES

Aki, K., 1967: Scaling law of seismic spectrum. *J. Geophys. Res.*, **72**, 1217-1231.

Beresnev, I. A., and G. M. Atkinson, 1997: Modeling finite-fault radiation from the ω^{-n} spectrum. *Bull. Seismol. Soc. Am.*, **87**, 67-84.

Bolt, B. A., 1986: Seismic Energy release over a broad frequency band. *Pure Appl. Geophys.*, **124**, 919-930.

Boore, D. M., 1988: The effect of finite bandwidth on seismic scaling relationships. in Earthquake Source Mechanics. *AGU Geophys. Mono.*, **27**, 275-283.

Brune, J. N., 1970: Tectonic stress and the spectra of seismic shear waves from earthquake. *J. Geophys. Res.*, **75**, 4997-5009.

Di Bona, M., and A. Rovelli, 1988: Effects of the bandwidth limitation on stress drops estimated from integrals of the ground motions. *Bull. Seismol. Soc. Am.*, **78**, 1818-1825.

Huang, M. W., and J. H. Wang, 2002: Scaling of displacement spectra of the 1999 Chi-Chi, Taiwan, earthquake from near-fault seismograms. *Geophys. Res. Lett.*, **29**, 47/1-4.

Huang, M. W., J. H. Wang, R. D. Hwang, and K. C. Chen, 2002: Estimates of source parameters of two large aftershocks of the 1999 Chi-Chi, Taiwan, earthquake in Chia-Yi area. *Terr. Atmos. Ocean. Sci.*, **13**, 299-312.

Hwang, R. D., J. H. Wang, B. S. Huang, K. C. Chen, W. G. Huang, T. M. Chang, H. C. Chiu, and C. C. Tsai, 2001: Estimates of stress drop from near-field seismograms of the M_s 7.6 Chi-Chi, Taiwan, earthquake of September 20, 1999. *Bull. Seismol. Soc. Am.*, **91**, 1158-1166.

Ide, S., and G. C. Beroza, 2001: Does apparent stress vary with earthquake size? *Geophys. Res. Lett.*, **28**, 3349-3352.

Singh, S. K., and M. Ordaz, 1994: Seismic energy release in Mexican subduction zone earthquakes. *Bull. Seismol. Soc. Am.*, **84**, 1533-1550.

Smith, K. D., J. N. Brune, and K. F. Priestley, 1991: The seismic spectrum, radiated energy, and Savage and Wood inequality for complex earthquakes. *Tectonophysics*, **188**, 303-320.

Wang, J. H., 2004: The seismic efficiency of the 1999 Chi-Chi, Taiwan, earthquake. *Geophys. Res. Lett.*, **31**, L10613, doi: 10.1029/204GL019417.

Wang, J. H., 2006: Energy release and heat generation during the 1999 Chi-Chi, Taiwan, earthquake. *J. Geophys. Res.*, **111**, B11312, doi: 10.1029/2005JB004018.

Wang, J. H., and M. W. Huang, 2007: Effect of finite frequency bandwidth limitation on evaluations of seismic radiation energy of the 1999 Chi-Chi Earthquake. *Terr. Atmos. Ocean. Sci.*, **18**, 567-576, doi: 10.3319/TAO.2007.18.3.567(T).